Resonance excitation of light field in weakly absorbing spherical particles by a femtosecond laser pulse. Peculiarities of nonlinear optical interactions

A.A. Zemlyanov and Yu.E. Geints

Institute of Atmospheric Optics,
Siberian Branch of the Russian Academy of Sciences, Tomsk

Received May 3, 2001

Based on the numerical solution of linear problem on diffraction of a femtosecond plane wave on a weakly absorbing spherical particle, the spatial and temporal structure of the light field inside a sphere is studied. It was found that there exists a multimode regime of excitation of whispering-gallery (WG) modes. The effect of the spectral width ratio between the excited WG mode and the laser pulse is analyzed. It is shown that the decrease of this ratio at transition from a monochromatic wave to a femtosecond pulse leads to a significant decrease of the high-intensity internal field at the points of its maxima. The possibility of obtaining stimulated radiation in a microparticle at the Stokes and third-harmonic frequencies is shown.

Introduction

The progress in technology of high-power femtosecond lasers far extends the applicability of a laser to environmental studies. Thanks to high intensity (~ $10^{13} - 10^{15}$ W/cm^2), ultrashort duration (several femtoseconds), and the wide spectral interval of such pulses,[1] new capabilities appear in diagnostics of gas–aerosol media with high spatial resolution and high sensitivity.[2,3]

By now, the first experiments have been conducted that have demonstrated high efficiency of femtosecond technologies in application to solving some problems in remote sensing of the atmosphere.[2]

A new research field – femtosecond atmospheric optics – is now being developed in atmospheric optics.[4] Within the framework of this topic, the problem of interaction of high-power femtosecond radiation with the aerosol component is of great interest. Excitation of different processes of stimulated scattering in microparticles allows chemical composition of aerosol particles to be analyzed and, in some cases, to determine their size spectrum.[5] Besides, theoretical and experimental works on nonlinear femtosecond optics of aerosol that are important for atmospheric optics also are of importance in the optics of microcavities and related spectroscopy of the particulate matter.

In nonlinear optics of aerosols in quasi-stationary light fields, the following processes of stimulated scattering were studied: stimulated Raman scattering (SRS), stimulated Brillouin scattering (SBS), and stimulated fluorescence (SF).[6,19] Experimental[7,8,10] and theoretical[8] results on the third harmonic generation (THG) in microparticles were also obtained.

In Ref. 7, it was found that THG arises in microparticles along with SBS under conditions of quasi-stationary excitation, and the resulting spectrum consists of separate lines from the lines of the third harmonic of q-order SRS (q = 1, 2, ...) $3\omega_{sq}$ to the line $3\omega_0$ (ω_0 is the fundamental laser frequency). For these conditions the efficiency of THG is low, and its intensity is usually ~ $10^{-4} - 10^{-6}$ of the SRS intensity.[8]

The third-harmonic signal from aerosol particles was observed in the experiment[10] from particles that were exposed to pulsed radiation from Ti:sapphire laser with the duration of 80 fs and the peak power of ~ 5.3 GW. The laser pulse repetition frequency was 1 kHz, and the laser wavelength centered near 820 nm. In the experiment, water droplets from 1 to 32 μm in size were used. The angular characteristics of radiation were studied as well. The experimental observation limit for the third-harmonic signal was $5 \cdot 10^{11}$ W/cm^2. The experimental data on the other important effect – SRS – stimulated by a femtosecond pulse in a particle are absent in the literature.

New results have been obtained recently in femtosecond nonlinear optics of extended media. They are of great interest for nonlinear optics of aerosols. For femtosecond pulses with the duration t_p shorter than the period of molecular vibrations in a matter T_R, SRS manifestation has some peculiarities as compared to that under the quasi-stationary conditions. As such a pulse propagates along the Raman-active medium, every its Fourier component is converted nonlinearly. This gives rise to conversion of the entire spectrum of the pulse – it shifts to the red region.[11,13]

The effect of pulse "clearing" of high-frequency components and conversion into an IR femtosecond pulse has been predicted in Ref. 14.

Another interesting fact has been discovered experimentally in Ref. 12. Stimulated molecular vibrations arose as a Raman-active medium was exposed to a group of femtosecond pulses with the repetition period equal to the period of molecular vibrations. The

0235-6880/01/05 316-10 $02.00

properties of stimulated molecular vibrations were studied from scattering of a probe light wave.

Obviously, the conditions of appearance of such effects in microparticles are different. This is connected with significantly different character of the spatiotemporal behavior of optical fields in a particle–microcavity as compared to the traveling waves.

An important feature of a femtosecond laser pulse is its wide spectrum. The width of the pulse spectrum $\Delta\omega_p$ is inversely proportional to the pulse duration t_p and can reach $\Delta\omega_p \sim 10^{15} - 10^{16}$ Hz at $t_p \approx 10^{-14} - 10^{-15}$ s. That wide frequency region allows obtaining excitation of a large number of high-Q resonance modes, the so-called whispering gallery (WG) modes, in a particle. The presence of these modes favors efficient nonlinear interaction of waves. The interaction time for optical fields in the WG modes increases significantly; for the case of traveling waves, this is equivalent to the increase of the distance at which they interact. Thus, strict restrictions imposed on tuning the frequency of the incident field to particle resonances are lifted by use of femtosecond pulses, and the efficiency of mode coupling at nonlinear interaction increases. In a microcavity, not all modes are under the same energy conditions, and only the WG modes can take an active part in the process.

An important stage in the research into nonlinear optical interactions in a microcavity is the study of resonance structure of the inner optical field. It is just this problem the solution of which this paper addresses to. In addition, it analyzes peculiarities of nonlinear interactions of optical fields of femtosecond pulses in a microparticle.

1. Optical field of ultrashort pulse in a dielectric sphere

The problem discussed is from the category of problems on diffraction of nonstationary and, in the general case, inhomogeneous light field on a dielectric sphere. The technique of solving such problems was considered in Refs. 15–17. Let us consider now the key items in the description of the transient stage in formation of the inner optical field in spherical dielectric particles in a linear formulation. The nonlinear effects will be estimated in Section 3. We assume the particle to be at the origin of coordinates, and the laser pulse diffracting on this particle propagates along the axis z. The strength of the electric field of incident radiation can be written as

$$\mathbf{E}_0(\mathbf{r};\, \tau) = 1/2\, E_0\, \mathbf{p}_e\, g(\tau)\, H(\mathbf{r}_\perp) \exp(i\omega_0\tau) + \text{c.c.}, \quad (1)$$

where $\omega_0 = 2\pi f_0$; f_0 is the carrier frequency of the pulse; E_0 is the real field amplitude; $g(\tau)$ and $H(\mathbf{r}_\perp)$ are the temporal and spatial pulse profiles, respectively; $\mathbf{r} = \mathbf{r}_\perp + \mathbf{e}_z z$; $\mathbf{e}_z$ is the unit vector along the z axis; $\tau = t - z/c$ is the time measured in the coordinate system moving with the light pulse (hereinafter, the "shifted" time); c is the speed of light; $\mathbf{p}_e$ is the vector determining the polarization of the light wave.

To calculate the distribution of the inner optical field of the particle and apply the apparatus of the Mie theory, one should first pass from the temporal coordinates to the domain of spectral frequencies by use of the Fourier transform of the initial light pulse

$$\mathbf{E}_0(\mathbf{r};\, \omega) = \int_{-\infty}^{\infty} \mathbf{E}_0(\mathbf{r};\, \tau) \exp(-i\omega\tau)\, d\tau =$$

$$= E_0\, \mathbf{p}_e\, H(\mathbf{r}_\perp)\, G(\omega - \omega_0), \quad (2)$$

where $G(\omega - \omega_0) = \int_{-\infty}^{\infty} g(\tau) \exp\{-i(\omega - \omega_0)\tau\}\, d\tau$ is the Fourier transform of the function $g(\tau)$. Similarly, by inverse transformation, we obtain

$$\mathbf{E}_0(\mathbf{r};\, \tau) = \frac{1}{2\pi} \int_{-\infty}^{\infty} \mathbf{E}_0(\mathbf{r};\, \omega) \exp(i\omega\tau)\, d\omega =$$

$$= \frac{1}{2\pi}\, \mathbf{p}_e\, H(\mathbf{r}_\perp) \int_{-\infty}^{\infty} E_0\, G(\omega - \omega_0) \exp(i\omega\tau)\, d\omega. \quad (3)$$

Formally, this equation determines the initial pulse as a sum of the infinite series of elementary monochromatic waves with the amplitudes $A(\omega) = E_0\, G(\omega - \omega_0)\, d\omega$. Every wave diffracts on the particle, thus making the contribution $A(\omega)\mathbf{E}_\delta(\mathbf{r};\, \omega)$ to the total amplitude of the internal field. The magnitude of this contribution depends on the optical properties of the particle, as well as on the spatial profile of the beam $H(\mathbf{r}_\perp)$; this is taken into account in the pulse response function (transfer function) of the particle–environment system $\mathbf{E}_\delta(\mathbf{r};\, \omega)$. Thus, the time-dependent strength of the electric field inside the particle $\mathbf{E}_i(\mathbf{r};\, \tau)$ can be expressed through the inverse Fourier transform of the product of the frequency spectrum of the initial pulse and the transfer function:

$$\mathbf{E}_i(\mathbf{r};\, \tau) = \frac{1}{4\pi} E_0 \exp(i\omega_0\tau) \times$$

$$\times \int_{-\infty}^{\infty} G(\omega)\, \mathbf{E}_\delta(\mathbf{r};\, \omega - \omega_0) \exp(i\omega\tau)\, d\omega + \text{c.c.} \quad (4)$$

The pulse response function $\mathbf{E}_\delta(\mathbf{r};\, \omega)$ can be determined from the stationary Mie theory by calculating the amplitude of the internal field of the particle exposed to a monochromatic light wave with the unit amplitude, frequency ω, polarization vector $\mathbf{p}_e$, and the spatial profile $H(\mathbf{r}_\perp)$. Thus, for example, in the spherical coordinate system $\mathbf{r} = (r, \theta, \varphi)$ the function $\mathbf{E}_\delta$ is described by the following equation[18,19]:

$$\mathbf{E}_\delta(\mathbf{r};\, \omega) = \frac{1}{2k_a r} \sum_{n=1}^{\infty} \sum_{m=-n}^{n} \Big\{ c_{nm}(x_a)\, \mathbf{M}_{nm}(\theta,\, \varphi)\, \psi_n(k_a r) +$$

$$+ \frac{1}{k_a}\, d_{nm}(x_a)\, \nabla \times [\mathbf{M}_{nm}(\theta,\, \varphi)\, \psi_n(k_a r)] \Big\} + \text{c.c.}, \quad (5)$$

where $k_a = \omega n_a / c$ is the wave number inside the particle; $m_a = n_a + i\iota_a$ is the complex refractive index; n_a is the real refractive index, ι_a is the absorption coefficient of the particulate matter; $m = m_a / m_0$ is the relative refractive index (m_0 is the refractive index of the environment); $x_a = k_a a_0 / n_a$ and a_0 are the diffraction parameter and the particle radius, respectively; $\mathbf{M}_{nm}$ are the spherical vector-harmonics; ψ_n and ξ_n are the spherical Ricatti–Bessel functions; c_{nm} and d_{nm} are the generalized Mie coefficients related to the known amplitudes of the partial waves of the internal field c_n and d_n for a plane wave[18] and the beam shape factors $(g_{nm})_{\mathrm{TE}}$ and $(g_{nm})_{\mathrm{TH}}$ for the TE and TH polarization, respectively, by the equation[20]:

$$c_{nm} = c_n (g_{nm})_{\mathrm{TH}}; \quad d_{nm} = d_n (g_{nm})_{\mathrm{TE}};$$

$$c_n = i^n \frac{2n+1}{n(n+1)} \frac{-m}{\xi_n'(x_a)\,\psi_n(mx_a) - m\,\xi_n(x_a)\,\psi_n'(mx_a)};$$

$$d_n = i^n \frac{2n+1}{n(n+1)} \frac{m}{\xi_n(x_a)\,\psi_n'(mx_a) - m\,\xi_n'(x_a)\,\psi_n(mx_a)}.$$

The coefficients g_{nm} depend only on the specific beam profile $H(\mathbf{r}_\perp)$ and the geometry of its incidence onto the particle.

Combining equations (4) and (5), we finally have for the envelope of the inner electric field strength:

$$\tilde{\mathbf{E}}_i(\mathbf{r};\tau) = \frac{1}{4k_a r} \sum_{n=1}^{\infty} \sum_{m=-n}^{n} \{[s_{nm}]_{\mathrm{TH}}\,\mathbf{M}_{nm}(\theta,\varphi) + \nabla \times [[s_{nm}]_{\mathrm{TE}}\,\mathbf{M}_{nm}(\theta,\varphi)]\} + \mathrm{c.c.}, \tag{6}$$

where $[s_{nm}]$ are the time-dependent partial amplitudes:

$$[s_{nm}]_{\mathrm{TH}} = \frac{1}{2\pi} \int_{-\infty}^{\infty} \frac{d\omega}{\omega^2}\, c_{nm}(\omega - \omega_0) \times \psi_n(\omega - \omega_0, r)\, G(\omega) \exp(i\omega\tau).$$

$$[s_{nm}]_{\mathrm{TE}} = \frac{c}{2\pi n_a} \int_{-\infty}^{\infty} \frac{d\omega}{\omega^2}\, d_{nm}(\omega - \omega_0) \times \psi_n(\omega - \omega_0, r)\, G(\omega) \exp(i\omega\tau). \tag{7}$$

In the numerical calculations of the evolution of the optical field intensity inside a particle, the temporal profile of the laser pulse was taken to be Gaussian:

$$g(\tau) = \exp\{-\tau^2 / t_{\mathrm{p}}^2\}, \tag{8}$$

where t_{p} is the pulse halfwidth at the level of e^{-1}. It was also assumed that the laser pulse is a plane wave polarized along the axis y, i.e., $\mathbf{p}_{\mathrm{e}}\, H(\mathbf{r}_\perp) = \mathbf{e}_y$. The case of diffraction of a spatially limited beam is beyond the scope of this paper. For the function (8), the Fourier transform is also Gaussian with the spectrum halfwidth $\Delta\omega_{\mathrm{p}} = 4\pi / t_{\mathrm{p}}$; therefore, it can be written as

$$G(\omega) = \frac{4\pi\sqrt{\pi}}{\Delta\omega_p} \exp\left\{-4\pi^2 \frac{\omega^2}{\Delta\omega_{\mathrm{p}}^2}\right\}. \tag{9}$$

2. Discussion

Calculations were performed in the following order. First, the laser pulse spectrum (9) was calculated at N_s points with the discretization step $\Delta\omega = 4\pi f_s$, where f_s is the discretization frequency. The number of nodes N_s was chosen so that the condition $N_s \Delta\omega / \Delta\omega_{\mathrm{p}} \geq 3$ be always fulfilled. Then we calculated partial amplitudes $[s_{nm}]$ by Eqs. (7) using specially developed Mie-theory-based software and summed them up according to Eq. (6) separately for every spherical component of the inner electric field $\tilde{\mathbf{E}}_i(\mathbf{r};\tau)$. Thus obtained values were used to construct a dimensionless combination giving the relative intensity of the internal field (inhomogeneity factor) $B(\mathbf{r};\tau) = \frac{1}{E_0^2} |\tilde{\mathbf{E}}_i(\mathbf{r};\tau)|^2$. Finally, the values of the obtained 4D B matrix were interpolated from the shifted time τ to the real time t with the use of the spline-approximation.

The particle size was tuned to a selected resonance mode by seeking the corresponding extreme in the amplitude coefficients c_n and d_n by use of the golden section method.[19] In all cases, the calculations were performed for water droplets with $n_a = 1.33$ suspended in air and the water refractive index $\iota_a = 10^{-8}$. The carrier frequency of the laser pulse was taken to be $f_0 = 5.64 \cdot 10^{14}$ Hz; this frequency corresponds to the wavelength $\lambda_0 = 0.532$ μm. The dispersion of the refractive index within the spectral interval chosen was neglected.

Before discussing the results obtained, let us consider the characteristic peculiarities in the spatial distribution of the light field of resonance modes of spherical particles. In the general case, the electromagnetic field inside a large transparent particle has a complicated spatial structure that is characterized by the presence of a number of spikes whose intensity may differ by 10 to 100 times. Intensity of the internal field is maximum near the surface of a sphere along the incidence direction of a light wave; these peaks correspond to the zones of incident wave focusing by the front and rear surfaces of the particle (Fig. 1*a*).

The resonance of the field inside the particle occurs when the frequency of incident wave is tuned to the frequency of one of the particle's natural modes. In this case, the spatial structure of the internal field transforms, thus leading to a sharp increase in the intensity within the focal zones (hundreds thousand times for high-Q resonances), and the field localizes near the surface of the spherical particle that leads to formation of the periodic ring structures in the form of standing waves (Fig. 1*b*). These near-surface resonance modes, as was mentioned above, are called the whispering-gallery modes.[21] From the viewpoint of the ray optics, the WG modes correspond to stable congruences of the rays refracted by the spherical surface, if the condition of the total internal reflection is fulfilled for them. These rays are as if captured by the particle and, passing along its surface, form a

closed zone limited by the inner caustic from the one side and the particle surface from the other side.[22]

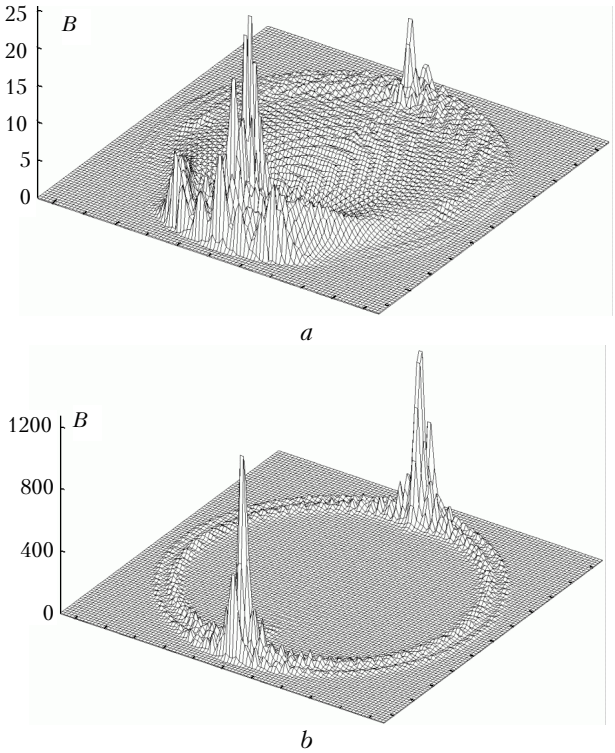

Fig. 1. Spatial distribution of the relative intensity of an optical field inside a water droplet with the radius $a_0 = 5$ μm irradiated by a plane wave with $\lambda = 0.532$ μm in the case of nonresonance scattering (*a*) and excitation of the resonance $TE_{70,2}$ mode (*b*).

Resonance modes of the spherical cavities are usually characterized by polarization of the light waves (TE or TH) and two integer indices: mode number n and its order l. The physical meaning of these indices becomes clear from Fig. 1*b*. The number of a mode is equal to the half number of the maxima of the internal field over the spherical angle θ, and the order number corresponds to the number of rings in the radial direction. This form of the field is a direct consequence of the fact that the internal field is presented as an expansion in terms of the particle's natural modes (5). In the case of a resonance, the term in the Mie series that has the corresponding polarization and number dominates. As this takes place, most of the energy of the resonance mode, as in the nonresonance case, localizes in the zones of the incident wave focusing that are related to each other by the ring structure of the WG mode.

Theoretically, the Q-factor of the WG modes of transparent spherical particles determined as the ratio of the light field energy stored in the mode to the total power loss in the cavity can be very high, especially, for low-order resonances. In practice, however, it is significantly limited by the absorption of the particulate matter, as well as by imperfections in the particle surface and nonlinearity of the refractive index n_a (see the review in Ref. 19). Therefore, the total (effective) Q-factor is usually used, and its value is determined as

$$1/Q = 1/Q_r + 1/Q_a , \qquad (10)$$

where Q_r and Q_a are the cavity Q-factors due to radiative losses and absorption, respectively. From this equation it is seen that the value of Q is determined by the smallest term.

The cavity Q-factor is closely connected with the characteristic lifetime of the resonance mode $\tau_r = Q/\omega$, which is roughly equal to $10^{-9} - 10^{-7}$ s at $Q \sim 10^6 - 10^8$ and the frequencies lying in the visible spectral region.

Figure 2 shows the dependence of the lifetime τ_r of different resonance modes (different mode indices and orders) on the particle diffraction parameter. Obviously, if the duration of the radiation pulse is less than the lifetime $t_p < \tau_r$, then the optical field exists in the particle even after the laser pulse terminates.

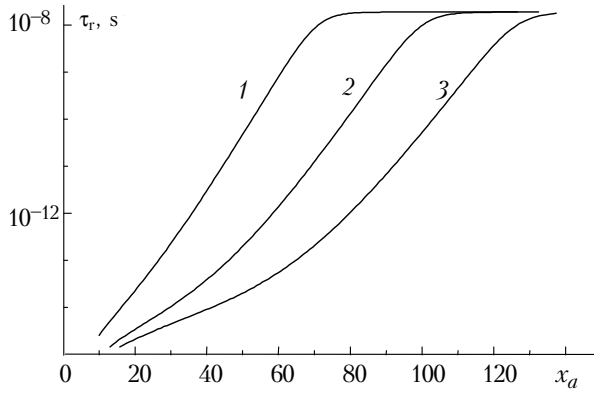

Fig. 2. Characteristic lifetime τ_r of different WG resonance modes excited in particles vs. diffraction parameter x_a of the particle. The curve numbers correspond to the order of resonance modes. Absorption of the particulate matter (water) is taken to be $\iota_a = 10^{-8}$.

The time dependence of the relative intensity of the optical field calculated for the $TE_{70,1}$ resonance in a water droplet with the radius $a_0 = 5.97003$ μm exposed to the radiation pulses with the durations $t_p = 100$ ps and $t_p = 10$ fs is shown in Fig. 3.

The factor B was calculated at three points corresponding to three characteristic areas inside the particle. They are the area of the absolute maximum of the field intensity (point *1*) in the shadow focal zone ($r/a_0 = 0.89$; $\theta = 0°$), the ring zone of the WG mode (point *2*) near the particle surface ($r/a_0 = 0.89$; $\theta = 90°$), and the zone of nonresonance background (point *3*) at the central area of the droplet ($r/a_0 = 0.40$; $\theta = 40°$). The time scale in Fig. 3 is normalized to the duration of the laser pulse, and the intensity is normalized to its maximum value in the particle volume.

It is seen from Fig. 3*a* that the time behavior of the optical field intensity at the points *1* and *2* has the pronounced resonance character and it decreases exponentially with the constant τ_r equal to ~0.6 ns for the $TE_{70,1}$ mode. At the same time, at the point *3* the intensity of the internal field follows the temporal profile of the laser pulse (shown by the dashed line). At a significantly shorter laser pulse (Fig. 3*b*), the character of these dependences changes.

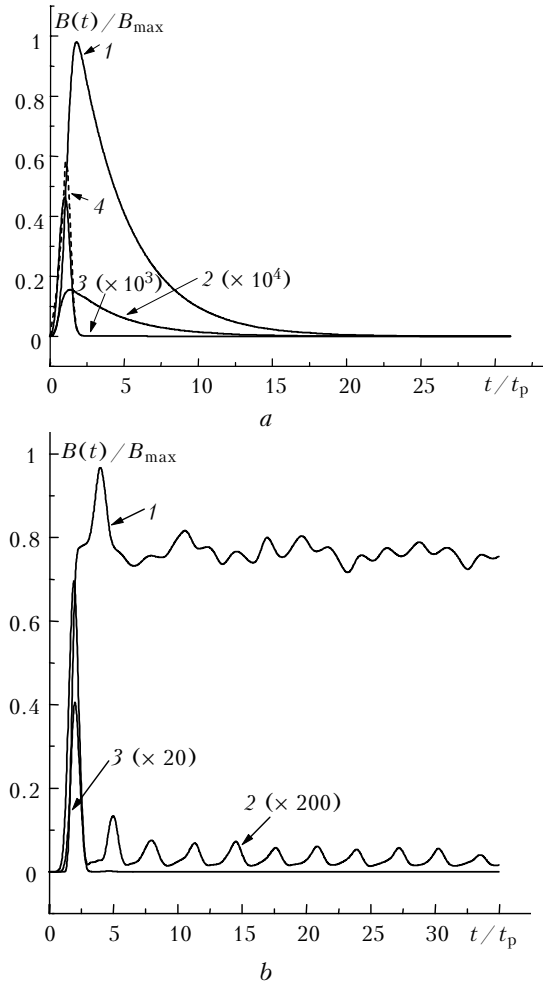

Fig. 3. The inhomogeneity factor (normalized to its maximum value) of the internal field as the $TE_{70,1}$ resonance mode is excited in the particle by a pulse with the duration t_p = 100 ps (*a*) and 10 fs (*b*). The plots are given for three points inside the particle: focal zone near the shadow surface (*1*), ring zone of WG mode (*2*), and the central zone (*3*). Curve *4* shows the temporal profile of the pulse (in rel. units).

First, instead of the smooth fall off in the resonance areas of the internal field, the intensity oscillates about some practically constant level. This is connected with the fact that the chosen interval of consideration (350 fs) is much shorter than the lifetime of the resonance mode τ_r, and its relative lifetime is long enough, $\tau_r/t_p \sim 6 \cdot 10^4$.

Second, the presence of the intensity oscillations in the resonance is the difference from the previous case. In the WG ring zone, these pulsations are regular, and their period correlates with the time needed for the pulse to travel round the particle surface $2\pi a_0$, which is equal to ~ 50 fs in the considered case. This circumstance indirectly confirms the physical interpretation of the resonances in particles as a standing wave formed by the interference between two in-phase waves propagating along the particle surface in the counter directions.

As follows from the principles of spectral analysis of signals, signal compression in time is accompanied by broadening of its frequency spectrum. As known, in the case of Gaussian time profile of the signal (8), the condition $(t_p\,\Delta\omega_p) = 4\pi$ is fulfilled. Consequently, at t_p = 100 ps the spectral halfwidth of the laser pulse is $\Delta\omega_p \approx 1.3 \cdot 10^{11}$ Hz, whereas at t_p = 10 fs $\Delta\omega_p$ it is already ~$1.3 \cdot 10^{15}$ Hz, i.e., comparable with the pulse carrier frequency ω_0. This leads to the situation that the spectral function of the pulse response $\mathbf{E}_\delta(\omega)$ from a particle, at short pulses, takes the form different from that in the case of a quasistationary excitation.

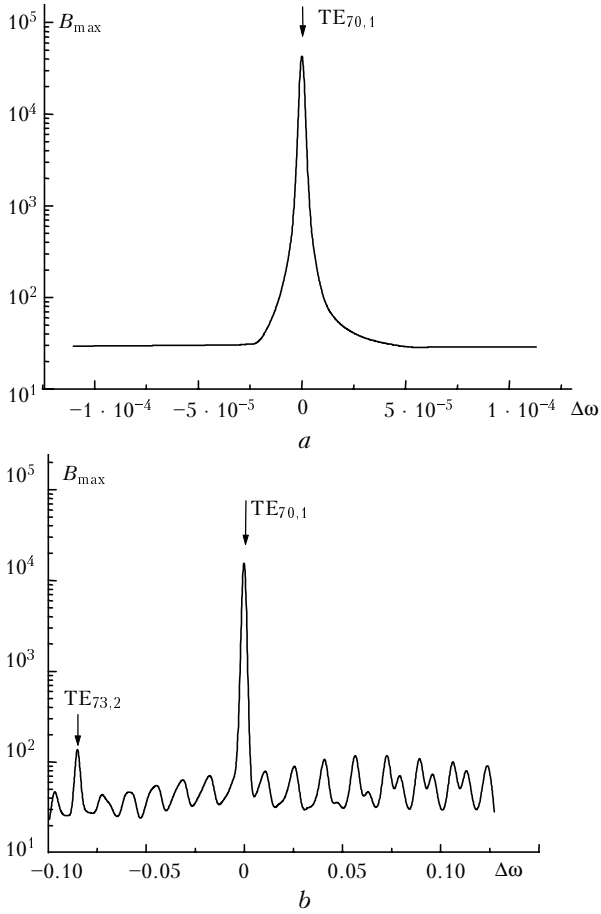

Fig. 4. The intensity of the internal field B_{max}, maximum all over the particle volume, as a function of the relative frequency detuning of the light wave $\overline{\Delta\omega}$. The upper and lower panels show two different situations with the laser pulses: t_p = 100 ps (*a*) and 10 fs (*b*). The arrows indicate the positions of the most intense resonance modes.

Figure 4 shows the intensity of the internal field B_{max}, maximum all over the particle volume, as a function of the relative detuning of the laser frequency from the resonance value $\overline{\Delta\omega} = (\omega - \omega_r)/\omega_r$. It should be noted that the range of the frequency detuning $\overline{\Delta\omega}$ in Fig. 4 is different – it reflects the spectral width of the diffracting pulse. It is seen from Figs. 4*a* and *b* that at t_p = 10 fs the pulse spectrum includes several quite intense resonances corresponding to the WG modes. On the other hand, at t_p = 100 ps the spectral width of the initial pulse is far narrower and contains only the central resonance mode ($\omega_r = \omega_0$).

Thus, the wide spectrum of a short pulse can simultaneously excite several WG modes in the particle. The fields of these modes overlap and thus cause the time dependence of the total field intensity in the zone of its maximum. This dependence manifests itself in the form of characteristic wave oscillations. The amplitude of these oscillations depends on the out-phasing of the resonance fields. Calculations show that an increase of the particle radius and the related closeness of the frequency modes, on the spectral scale, lead to a decrease in the amplitude of the observed intensity oscillations.

Using the Mie theory and the ray asymptotic of the WG,[22,23] we can estimate the mean number of resonances that can be excited simultaneously in the particle exposed to the radiation pulse with the spectral halfwidth $\Delta\omega_p$. To do this, we introduce the term of the spectral density of the resonance modes $f_m(\omega)$ as the number of most intense resonances (of both polarizations) within a unit frequency interval:

$$f_m(\omega) = \frac{2\omega_0 a_0}{\pi c} (n_a^2 - 1)^{1/2} \left[\frac{(n_a^2 - 1)^{1/2}}{\arctan \{(n_a^2 - 1)^{1/2}\}} - 1 \right]. \quad (11)$$

Only those resonance modes are taken into account here, whose field is concentrated inside the so-called transient zone[23] limited by the inner caustic with the radius $r_c = (n + 1/2)\, c/\omega_0$. The inner caustic, in its turn, is formed by the rays incident on the inner surface of the particle at the angle of total internal reflection.

Integrating Eq. (11) over the frequency interval $2\Delta\omega_p$, we obtain the total number of the WG modes in the particle N_m:

$$N_m = \int\limits_{2\Delta\omega_p} f_m(\omega')\mathrm{d}\omega' \approx K(n_a) \frac{a_0}{c^2} \omega_0^2 \left(\frac{\Delta\omega_p}{\omega_0} \right), \quad (12)$$

where $K(n_a) \approx 0.416\ (n_a^2 - 1)^{1/2}\ (n_a - 1)$, $1 < n_a < 2$.

Figure 5 shows the number of resonances N_m as a function of the pulse duration t_p connected with $\Delta\omega_p$ by Eq. (9) for the particles of different radius. It is seen from the figure that the pulses of pico- and subpicosecond duration can induce multimode excitation only in large particles, whereas small particles ($a_0 < 1$ μm), because of their low resonance properties, are capable of maintaining only one resonance mode almost in the entire range of the pulse duration. The fact that for such particles $N_m < 1$ is not an error. It indicates that resonance excitation of small particles is possible only in the case of special tuning of the frequency of the incident radiation to the resonance. At the same time, at $N_m \gg 1$ the optical field inside the particles is always in resonance with a number of WG modes. Since these natural modes are independent, they all can be maintained by the incident radiation. Note, however, that the competition between different resonance modes is always present, and the main factors responsible for the competitive selection include the effective Q-factor of the mode [Eq. (10)] and detuning of a WG mode ω_r from the central frequency of the laser pulse spectrum ω_0.

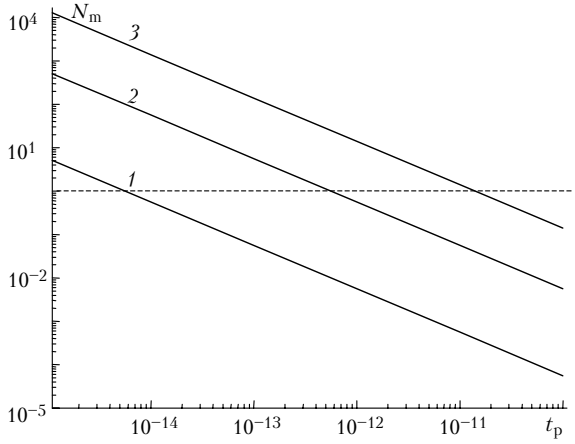

Fig. 5. The mean number N_m of the resonance WG modes, which can be excited simultaneously in particles of different radius $a_0 = 1$ (*1*), 10 (*2*), and 50 μm (*3*) exposed to laser pulses with the duration t_p. The dashed line corresponds to the level $N_m = 1$.

It is also interesting, in studying the resonance field excitation in particles by ultrashort pulses, to study the maximum possible level of focusing of the internal field as compared to the laser pulse intensity. In other words, this means the dependence of the maximum values of the inhomogeneity factor B_{max} of the internal field in the resonance mode on the laser pulse duration. This problem is important, because the factor B plays one of the key roles in the processes of nonlinear interaction of waves in the microcavities, by affecting directly the efficiency of their coupling.[19]

As follows from the above-said, the peak of the internal field intensity is located near the shadow surface of the particle and this is caused by the focusing properties of spherical surface. Since the frequency spectrum of the laser pulse $\Delta\omega_p$ and the spectrum of the WG modes $\Delta\omega_r = \omega_r/Q$ have finite width, the efficiency of excitation of these resonance modes is determined, finally, by the ratio of these parameters. If the exciting pulse has a narrow spectrum, such that $\Delta\omega_p \ll \Delta\omega_r$ (conditions of long pulses or continuous emission), then its energy is completely transferred to the resonance mode. In the opposite case $\Delta\omega_p \gg \Delta\omega_r$ (short pulses), the WG mode perceives only a part of the pulse energy, which is transferred by the spectral components from the frequency region $\omega_0 - \Delta\omega_r/2 \le \omega \le \omega_0 + \Delta\omega_r/2$. The intensity of the internal field and, consequently, the efficiency of resonance excitation decrease in this case.

This reasoning is illustrated by Fig. 6, which shows the dependence of the maximum inhomogeneity factor B_{max} on the parameter $\gamma = (\Delta\omega_r/\Delta\omega_p)$ at excitation of different resonance modes in spherical particles. In this figure, one can see the transient zone in the dependences plotted with the center near $\gamma = 1$. The decrease of B_{max} with the shortening of pulse duration (decrease of the parameter γ) starts in this zone. This tendency becomes even more obvious, if the curves are normalized to the corresponding value of B_{max} for every resonance that is achieved in the limit of

continuous-wave radiation $t_p \to \infty$. The result of such normalization is shown in Fig. 7. To be noticed in the first turn is the fact that as the parameter γ varies in the range $0.1 \le \gamma \le 10$, all the curves drawn for different WG modes converge into a single dependence having the characteristic exponential drop profile. If we again pass from the spectral domain to the temporal scales, then the inequality $t_p > t_r$ corresponds to the condition of efficient excitation of resonances in the particle $\gamma > 1$. Thus, by analogy with the linear case of interaction of traveling waves, we can assert that the longer is the time of interaction of the basic wave with the field of the resonance mode in the spherical cavity, the more efficient is the energy transfer.

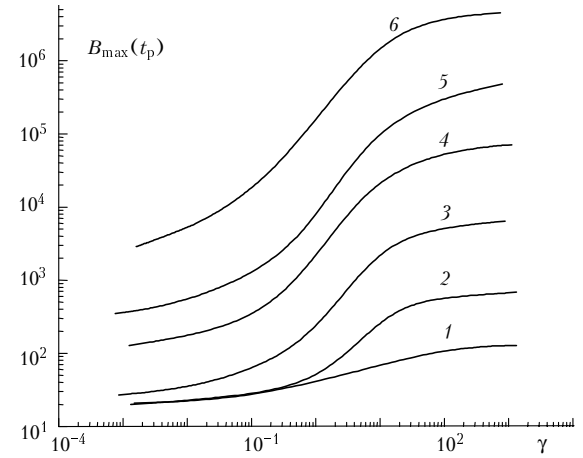

Fig. 6. Maximum inhomogeneity factor B_{max} of the optical field of resonance modes excited in a particle as a function of the frequency halfwidth ratio of these modes to the laser pulse γ. The following modes are shown: $TE_{85,3}$ (*1*), $TE_{70,2}$ (*2*), $TE_{85,2}$ (*3*), $TE_{100,2}$ (*4*), $TE_{70,1}$ (*5*), and $TE_{85,1}$ (*6*).

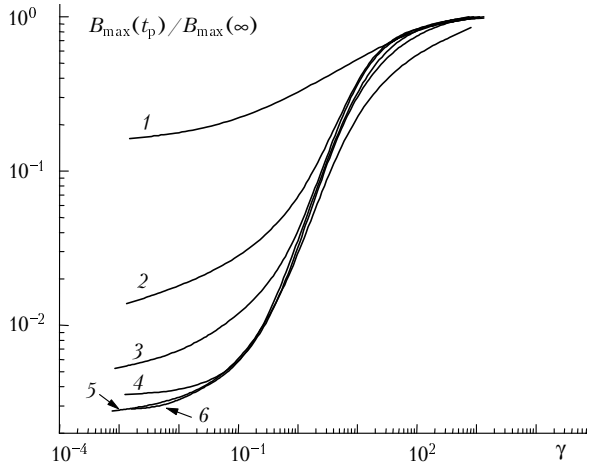

Fig. 7. The same as in Fig. 6, but the inhomogeneity factor B_{max} is normalized to the level achieved in the limit of continuous-wave radiation ($t_p \to \infty$) for every resonance.

As noted above, the consequence of the pulse spectrum broadening is simultaneous excitation of several resonance modes in a particle. Multimode excitation leads, on the one hand, to temporal oscillations of the total intensity of the internal field (see Fig. 3*b*) and, on the other hand, to some its increase due to the contribution of different modes at spatial overlapping of their fields (just this is observed in Fig. 7 at $\gamma \ll 1$). The longer is the lifetime of the central WG mode (mode with the frequency ω_0), the smaller is this contribution.

Comparison of the dependences of field intensity in different spatial zones of the resonance mode on the parameter γ demonstrates that the decrease in the laser pulse duration has practically no effect on the intensity of the internal field in the near-surface ring zone of the WG mode (point *2* in Fig. 3), whereas in the focal zones the field intensity changes, for example, for the $TE_{70,1}$ mode by almost three orders of magnitude (see Fig. 8). This is explained by the fact that almost the whole energy of the resonance mode is concentrated in the zone of the absolute field maxima. Therefore, the outflow of the light field energy from the central resonance mode to the neighboring modes, which are excited not that efficiently, affects most strongly just the zone of the field maximum.

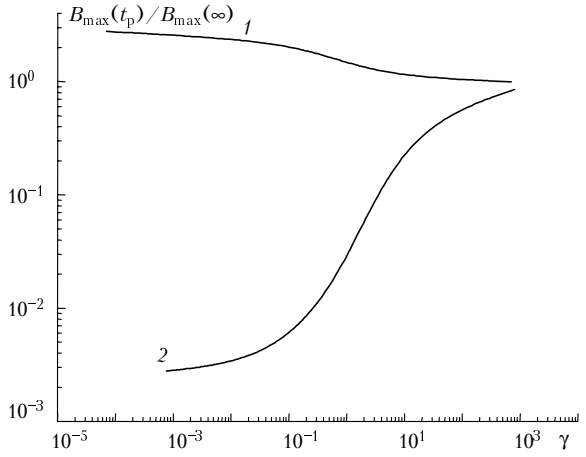

Fig. 8. Relative intensity of the optical field in different spatial zones of the $TE_{70,1}$ resonance mode as a function of the parameter γ: focal zone near the shadow surface of the particle (*1*) and ring zone of the WG mode (*2*).

3. Peculiarities of the nonlinear interactions of optical fields of femtosecond pulse in a microparticle

It was noted in the previous section that, owing to wide spectrum of a femtosecond laser pulse inside a microparticle, multiple WG modes can be excited inside it, that is, the multimode excitation of resonance modes can occur. The modes can generate nonlinear waves in different spectral regions.

Let us first write the most general equation characterizing nonlinear optical interactions in the particulate matter. The effects of nonlinear optics of ultrashort pulses are connected with the presence of the third-order nonlinear polarization of the medium.[1] The corresponding real vector of nonlinear polarization $\mathbf{P}_{nl}$ can be presented in the following form[24]:

$$\mathbf{P}_{\rm nl} = N_0\, Q_{\rm m}\, \mathbf{E} + \hat{\chi}_{\rm e}^{(3)}\, \mathbf{EEE}. \qquad (13)$$

In Eq. (13) the first term is responsible for the contribution from Raman scattering to nonlinear polarization of the medium, and the second term describes the contribution due to the electronic polarizability leading to the third harmonic generation. The designations are the following: $\mathbf{E}$ is the real vector of the electric field in the medium; N_0 is the number of molecules in a unit volume; $Q_{\rm m}$ is the coordinate of nuclei displacement in a molecule; $\hat{\chi}_{\rm e}^{(3)}$ is the tensor of third-order electronic susceptibility of the matter. For a fluid, the role of the second-order susceptibility leading, in particular, to the second harmonic generation is very small. Note that the electronic susceptibility follows the field almost immediately. At the same time, the SRS effect occurs in a certain delay.

Nonlinear polarization is the source of nonlinear optical waves in the particle. The equation for the electric field has the form

$$\text{rot rot}\, \mathbf{E}(\mathbf{r},\, t) + \frac{\varepsilon_a}{c^2}\frac{\partial^2 \mathbf{E}(\mathbf{r},t)}{\partial t^2} + \frac{4\pi\sigma}{c^2}\frac{\partial \mathbf{E}(\mathbf{r},t)}{\partial t} =$$

$$= -\frac{4\pi}{c^2}\frac{\partial^2}{\partial t^2}\mathbf{P}_{\rm nl}(\mathbf{r},\, t), \qquad (14)$$

where ε_a and σ are the dielectric constant and conductivity of the particulate matter, respectively. The medium is assumed homogeneous inside the particle. The coordinate $Q_{\rm m}$ is determined by the equation of forced vibrations:

$$\frac{\partial^2 Q_{\rm m}}{\partial t^2} + \frac{2}{T_2}\frac{\partial Q_{\rm m}}{\partial t} + \Omega_R^2\, Q_{\rm m} = F(t), \qquad (15)$$

where $F(t) = \dfrac{1}{2m}\dfrac{\partial \alpha}{\partial Q_{\rm m}} n_{\rm m} |\mathbf{E}|^2$ is the force; α is the medium polarizability; m is the molecular mass; T_2 is the time of cross relaxation; Ω_R is the frequency of molecular vibrations; $n_{\rm m} = (N_1 - N_2)/N_0$, $N_{1,2}$ are populations of the levels involved in the Raman active transition $1 \to 2$. The equation for $n_{\rm m}$ has the following form:

$$\frac{\partial n_{\rm m}}{\partial t} + \frac{n_{\rm m} - 1}{T_1} = \frac{1}{2\hbar\, \Omega_R}\frac{\partial \alpha}{\partial Q_{\rm m}}\, |\mathbf{E}|^2\, \frac{\partial Q_{\rm m}}{\partial t}, \qquad (16)$$

where T_1 is the time of longitudinal relaxation; $\hbar$ is the Planck's constant.

The solution for the coordinate $Q_{\rm m}$ is well known:

$$Q_{\rm m} = \frac{1}{2m}\frac{\partial \alpha}{\partial Q_{\rm m}} \exp(-t/T_2) \times$$

$$\times \int_0^t F(t') \exp(t'/T_2)\, \sin\Omega_R (t - t')\, {\rm d}t'. \qquad (17)$$

A peculiarity of the behavior of the coordinate $Q_{\rm m}$ in the microparticle is that, due to the excitation of WG modes in it, the characteristic properties of ultrashort pulses ($t_{\rm p} \ll T_2$ or $t_{\rm p} < \Omega_R^{-1}$) in no way do manifest themselves. This is connected with the fact that time behavior of the function F for the WG modes is determined by the modes' lifetimes rather than by the duration of a femtosecond laser pulse, as for the case of propagation of a traveling wave.

Our consideration is based on the physical model, in which whispering-gallery modes are formed as the pulse passes through the particle (for the time $\tau_{\rm r} \sim 2\pi a_0/c$), whereas no significant processes of nonlinear scattering occur in the particulate matter. If the modes formed by the femtosecond pulse include such that their frequencies ω meet the condition of Raman resonance $\omega_S \approx \omega_L - \Omega_R$, then the process of amplification of one mode with the frequency ω_S by the other mode with the frequency ω_L becomes possible.

For the time moment $t > t_{\rm p}$ the intensity in the WG mode, in the absence of a nonlinearity, can be presented as

$$I_{\rm WG}(\omega_{L,S}, t) = I_{\rm WG}(\omega_{L,S}, t_{\rm p}) \exp\{-(t - t_{\rm p})\, \omega_{L,S}/Q_{L,S}\}. \qquad (18)$$

Here $Q_{L,S}$ are the Q-factors for the corresponding modes, and they can be determined by Eq. (10). Since the lifetime of the modes is $\tau_{\rm r} \sim 10^{-9} - 10^{-7}$ s, the process of nonlinear interaction among the modes for such times can be considered in the quasistationary approximation. In this case, nonlinear polarization connected with the SRS process is formed in the medium. The vector of nonlinear polarization can be written as

$$\mathbf{P}_R^{(3)}(\omega_S) = \chi_R^{(3)}(\omega_S)\, (\tilde{\mathbf{E}}_L\, \tilde{\mathbf{E}}_L^*)\tilde{\mathbf{E}}_S + \text{c.c.} \qquad (19)$$

In Eq. (19), $\tilde{\mathbf{E}}_{L,S}$ are complex electric fields of the modes L and S; $\chi_R^{(3)}(\omega_S)$ is nonlinear susceptibility of the medium for the SRS effect. Under conditions of SRS resonance

$$\chi_R^{(3)} = -\, i\, \frac{N_0\, T_2}{16 m \Omega_R}\left(\frac{\partial \alpha}{\partial Q_{\rm m}}\right)^2. \qquad (20)$$

The equations describing mode interaction at SRS in a microparticle were derived in Ref. 25 in the quasistationary approximation. We use here these results, as well as the approximation of the given field of the pump mode. For the intensity of the Stokes mode we have

$$I_{\rm WG}(\omega_S,\, t_{\rm p}) = I_{\rm WG}(\omega_S,\, t_{\rm p}) \times$$

$$\times \exp\left\{\int_{t_{\rm p}}^{t} g\, I_{\rm WG}(\omega_L,\, t')\, {\rm d}t' - \frac{(t - t_{\rm p})\, \omega_S}{Q_S}\right\} \approx$$

$$\approx I_{\rm WG}(\omega_S,\, t_{\rm p}) \exp\left\{\frac{g\, I_{\rm WG}(\omega_L,\, t_{\rm p})\, Q_L}{\omega_L} \times\right.$$

$$\left. \times [1 - \exp\{-(t - t_{\rm p})\, \omega_L/Q_L\}] - \frac{(t - t_{\rm p})\omega_S}{Q_S}\right\}, \qquad (21)$$

where $g = \dfrac{c g_{\rm s} B_{\rm c}}{n_a}$, $g_{\rm s} = \dfrac{2\pi\, N_0\, \omega_S\, T_2}{c^2 \varepsilon_a\, m \Omega_R}\left(\dfrac{\partial \alpha}{\partial Q_{\rm m}}\right)^2$ is the coefficient of the Stokes wave intensification; $B_{\rm c}$ is the

coefficient of spatial overlapping of the fields of the modes L and S (Ref. 19).

Equation (21) shows that SRS leads to a decrease in the damping factor of the Stokes mode. The maximum intensification increment that is possible in the mode of the Stokes frequency can be expressed as follows:

$$G_{\max} = \frac{c g_s B_c I_{WG}(\omega_L, t_p) Q_S}{n_a \omega_S}. \qquad (22)$$

Let us assume that $I_{WG} \approx I_0 \frac{\Delta\omega_L}{\Delta\omega_p}$, where I_0 is the maximum intensity in the femtosecond pulse. The width of the WG modes is $\Delta\omega_L = \omega_L / Q_L$. Thus, we obtain

$$G_{\max} = \frac{c g_s B_c I_0 Q_S \omega_L \tau_p}{n_a \omega_S Q_L 4\pi}. \qquad (23)$$

The value of $G_{\max}$ depends significantly on the degree of spatial overlapping of the modes – the coefficient B_c. To estimate it reliably, additional investigations are needed. Assuming that $B_c = 1$, for $\omega_L = 3542$ THz, $\omega_S = 2898$ THz, $g_s = 10^{-3}$ cm/MW, $Q_S = Q_L$, and $\tau_p = 10$ fs, we have that $G_{\max} = 1$ at $I_0 \approx 5 \cdot 10^{13}$ W/cm^2. Such intensity levels are typical of the experiments on scattering of high-power femtosecond pulses on water particles.[10]

Let us consider how the field of the third harmonic (TH) is formed in a spherical particle under the effect of a femtosecond pulse. As a pulse of this duration passes through a particle, nonlinear polarization of the medium occurs at the triple frequency of every harmonic in the radiation spectrum. This polarization is the source of TH waves. If some Fourier component of the pulse spectrum is in resonance with a WG mode, then efficient nonlinear interaction between this component and the field of its TH is possible, if the TH is also the WG mode. Under such an interaction, a part of energy of the initial pulse is converted into the TH during the time the field exists in the particle. Thus, in contrast to the SRS, when the pulse itself contains components with the frequencies, whose difference is equal to the frequency of molecular vibrations, for the THG process the mode at the same frequency must be formed. To estimate the process of formation of the WG mode, we can use the approximation of the traveling wave.[26] For the intensity of TH that is generated as the pulse passes through the particle, we can write

$$I_3 = 576\pi^6 / n_a^4 \lambda_L^3 c^2 |\chi_{eg}^{(3)}|^2 I_0^3 L^2. \qquad (24)$$

Here L is the path length along the particle surface $L \approx 2\pi a_0$; $\chi_{eg}^{(3)}$ is the component of the tensor $\hat{\chi}_e^{(3)}$ responsible for the TH generation. The estimates by Eq. (24) indicate that for particles with the radii $a_0 \sim 10$ μm the experimentally measurable signal I_3 can be achieved.

Consider the relation between the contributions due to the SRS and the THG to the distortion of the pulse spectrum. If the modes maintaining the SRS and TH overlap, then the competition is possible between these effects. To determine what effect prevails in the nonlinear interaction, we use the quasistationary approximation. In this approximation, the parameter characterizing the relation between the components of nonlinear susceptibility, which determine the contributions to the nonlinear polarization coming from the effects of forced molecular vibrations and nonlinear electronic polarizability, is as follows[24]:

$$\delta = \frac{|\mathrm{Im}\, \chi_R^{(3)}|}{|\chi_{eg}^{(3)}|} = \frac{N_0}{48m} \left(\frac{\partial\alpha}{\partial Q_m}\right)^2 \frac{T_2}{\Omega_R} \Big/ |\chi_{eg}^{(3)}|.$$

For water δ is equal to 0.65 (Ref. 24). This value points to the fact that in water particles the contribution coming from electronic polarizability to the process of nonlinear interaction is somewhat larger than that from the SRS.

From the above physical consideration it follows that generation of high-Q components of the light field caused by nonlinear electronic polarizability as well as of the Stokes frequencies initiated by the stimulated Raman scattering is possible for the femtosecond pulse in a microparticle. A more accurate relation between the contributions from these two processes to the general pattern can be determined from a rigorous solution of the problem with the allowance made for the spatial and frequency interaction of the exciting and scattered fields; this solution will be considered in the future.

It is obvious that exposing the particle to a group of femtosecond pulses with the period $T_0 < \tau_r$, where τ_r is the characteristic lifetime of the mode taking part in a nonlinear interaction, we can obtain quasistationary excitation of stimulated emission. This distinguishes the pulsed interactions of a femtosecond pulse with a particle and the interaction with an extended medium, since in the latter case it is important for the pulse repetition frequency to be comparable with the frequency of molecular vibrations of the medium.

Conclusion

The studies conducted in this work allows the following conclusions to be drawn:

1. Excitation of resonance modes of the optical field in weakly absorbing spherical particles by femtosecond-duration pulses of radiation has some peculiarities as compared with the case of long pulses (or continuous-wave radiation). These peculiarities include the decrease of the resonance intensities of the internal field, especially in the zones of filed maximum (near the illuminated and shadow surfaces of the particle) and the occurrence of multimode excitation of resonance modes.

2. The efficiency of energy transfer from the incident light wave to the field of a resonance mode depends on the ratio between the spectral widths of the resonance mode being excited and of the laser pulse. The smaller is this ratio, as compared to the monochromatic wave, the less efficient is the excitation of resonances, and the intensity of the internal field in the zones of field maximum decreases.

3. The nonlinear optical effects of the SRS and THG in microparticles under the action of a high-power femtosecond pulse can occur in two stages. At the first one (transient stage), whispering-gallery modes are formed. At the second (quasistationary) stage, quasistationary generation of stimulated radiation in the Stokes and higher frequency, corresponding to the third harmonic, spectral regions is possible independent of the pulse duration.

Acknowledgments

The work was partially supported by the SB RAS Complex Integration Project No. 8 and the Russian Foundation for Basic Research Grant No. 01–02–16908.

References

1. C.A. Akhmanov, V.A. Vysloukh, and A.S. Chirkin, *Optics of Femtosecond Pulses* (Nauka, Moscow, 1988), 312 pp.
2. P. Rairoux, H. Schillinger, S. Niedermeier, et al., Appl. Phys. **B71**, 573–580 (2000).
3. V.M. Gordienko, A.I. Kholodnykh, and V.I. Pryalkin, Kvant. Elektron. **30**, No. 9, 839–842 (2000).
4. V.P. Kandidov, O.G. Kosareva, E.I. Mozhaev, and M.P. Tamarov, Atmos. Oceanic Opt. **13**, No. 5, 394–401 (2000).
5. J. Kasparian and J-P. Wolf, Opt. Commun. **152**, 355–360 (1998).
6. G. Schweiger, J. Aerosol Sci. **21**, No. 4, 483–509 (1990).
7. W.P. Acker, D.H. Leach, and R.K. Chang, Opt. Lett. **14**, No. 8, 402–404 (1989).
8. D.H. Leach, R.K. Chang, W.P. Acker, and S.C. Hill, J. Opt. Soc. Am. **B10**, No. 1, 34–45 (1993).
9. S.C. Hill, D.H. Leach, and R.K. Chang, J. Opt. Soc. Am. **B10**, No. 1, 16–33 (1993).
10. J. Kasparian, B. Krämer, T. Leisner, P. Rairoux, V. Boutou, B. Vezin, and J.P. Wolf, J. Opt. Soc. Am. **B15**, No. 7, 1918–1922 (1998).
11. Y.-X. Yan, E.B. Gamble, and K.A. Nelson, J. Chem. Phys. **85**, No. 11, 5391–5399 (1985).
12. A.M. Weiner, D.E. Leaird, G.P. Wiederrecht, and K.A. Nelson, J. Opt. Soc. Am. **B8**, No. 6, 1264–1275 (1991).
13. E.M. Belenov, A.V. Nazarkin, and I.P. Prokopovich, Pis'ma Zh. Eksp. Teor. Fiz. **55**, No. 4, 223–227 (1992).
14. A. Nazarkin and G. Korn, Phys. Rev. A **58**, No. 1, R61–R64 (1998).
15. V.E. Zuev, *Propagation of Visible and Infrared Waves in the Atmosphere* (Sov. Radio, Moscow, 1970), 497 pp.
16. D.Q. Chowdhury, S.C. Hill, and P.W. Barber, J. Opt. Soc. Am. **A9**, No. 8, 1364–1373 (1992).
17. K.S. Shifrin and I.G. Zolotov, Appl. Opt. **33**, No. 9, 7798–7804 (1994).
18. K.S. Shifrin, *Light Scattering in Turbid Medium* (Gos. Izdat. Tekhniko-Teor. Lit., Moscow, Leningrad, 1951), 288 pp.
19. Yu.E. Geints, A.A. Zemlyanov, V.E. Zuev, A.M. Kabanov, and V.A. Pogodaev, *Nonlinear Optics of Atmospheric Aerosol* (SB RAS Publishing House, Novosibirsk, 1999), 260 pp.
20. A.A. Zemlyanov and Yu.E. Geints, Atmos. Oceanic Opt. **13**, No. 5, 412–422 (2000).
21. V.M. Babich and V.S. Buldyrev, *Asymptotic Methods in Problems of Diffraction of Short Waves* (Nauka, Moscow, 1972), 295 pp.
22. G. Roll and G. Schweiger, J. Opt. Soc. Am. **A17**, No. 7, 1301–1311 92000).
23. P. Chýlek, J. Opt. Soc. Am. **7**, No. 7, 1609–1613 (1990).
24. C.A. Akhmanov and N.I. Korotaev, *Methods of Nonlinear Optics in Spectroscopy of Light Scattering* (Nauka, Moscow, 1981), 544 pp.
25. A.A. Zemlyanov and Yu.E. Geints, Atmos. Oceanic Opt. **12**, No. 10, 895–904 (1999).
26. G. Rogers, *Nonlinear Parametric Processes in Liquids and Gases* [Russian translation] (Mir, Moscow, 1987), 510 pp.